

Influence of Low Frequency Noise on Macroscopic Quantum Tunneling in Superconducting Circuits

Mathias Duckheim^{1,†*} and Joachim Ankerhold^{1,2}

¹*Physikalisches Institut, Albert-Ludwigs-Universität Freiburg,
Hermann-Herder-Straße 3, D-79104 Freiburg, Germany,*

²*Quantronics group, Service de Physique de l'Etat Condensé,
DSM/DRECAM, CEA Saclay, 91191 Gif-sur-Yvette, France*

(Dated: March 23, 2022)

The influence of low to moderate frequency environments on Macroscopic Quantum Tunneling (MQT) in superconducting circuits is studied within the $\text{Im}F$ approach to evaluate tunneling rates. Particular attention is paid to two model environments, namely, a pure sluggish bath and a sluggish bath with additional $1/f$ noise. General findings are applied to Zener flip tunneling, a MQT phenomenon recently predicted and observed in a superconducting circuit implementing a quantum bit.

PACS numbers: 74.50.+r, 05.40.-a, 85.25.Cp, 03.67.Lx

I. INTRODUCTION

The decay of a metastable system through macroscopic quantum tunneling (MQT) has been studied in view of conceptual questions in quantum theory already in the 1980s [1, 2]. Recently, it has regained new interest e.g. in the context of quantum information processing in solid state based systems [3, 4] or as an effective detection mechanism in shot noise measurements [5]. In corresponding electrical circuits, current-biased Josephson junctions are used as building blocks where the phase difference across a junction is the only relevant degree of freedom. The switching from the zero voltage state can then be visualized as the dynamics of a fictitious particle moving in a cubic potential such that at low temperatures the escape is dominated by quantum tunneling through the potential barrier. The crucial impact of the electromagnetic environment on this process has already been elucidated twenty years ago and then led to the development of the "standard" theory of quantum dissipative systems [6].

To date, the most powerful approach to calculate tunneling rates in dissipative systems is the so-called $\text{Im}F$ -method which relates the escape rate to the imaginary part of the free energy of an unstable system [1, 7]. Basically, it can be seen as the generalization of the method to extract the lifetime of an unstable state from an imaginary part of its resonance energy [8]. The theoretical predictions of the $\text{Im}F$ theory including dissipation [9] have been thoroughly tested in the 1980s in Josephson junction circuits [2]. In these studies the dominant effect of friction was due to dynamical environmental modes with ohmic spectral density. These modes generate at very low temperatures T a rate enhancement proportional to T^2 as compared to the zero temperature limit [10, 11].

In recent experiments with superconducting circuits

for the implementation of quantum bits, the role of low frequency modes in the environmental spectrum has turned out to be substantial [12, 13, 14, 15, 16]. Bath modes that are inert on the typical experimental time scales or show only slow to moderate dynamics basically determine the dephasing time for oscillations of coherent superpositions of qubit states. In many cases, the corresponding noise spectrum displays a $1/f$ dependence over a broad frequency range attributed e.g. to low frequency bistable charge fluctuators or electromagnetic fluctuations in control lines. In fact, $1/f$ noise has been known for years to be always present in mesoscopic devices [17, 18]. While detailed theoretical studies on its influence on the decoherence process in qubit devices have been given, apart from some qualitative estimates, much less is known about its impact on MQT.

In this paper, we analyse MQT processes subject to noise from very low up to moderate frequencies. One may expect that quantum fluctuations in the bath are thus suppressed. For two model environments, namely, a pure sluggish bath and an environment with $1/f$ characteristic, we show in detail to what extent this is actually true and how such a situation is incorporated into the $\text{Im}F$ theory. These findings are further applied to a particular kind of MQT phenomenon which has been predicted [19] and observed [20] recently in the so-called quantronium circuit [4]. This system, a superconducting circuit implementing a two-level system (qubit) with a readout by MQT, realizes an extension of the standard MQT scenario: It describes a fictitious particle with a spin- $\frac{1}{2}$ as an internal degree of freedom such that the Zeeman splitting of its levels is position dependent; in certain ranges of parameter space the Zeeman levels cross under the barrier leading to spin flips while tunneling. The MQT rate is then substantially enhanced since effectively the particle has to penetrate a smaller barrier.

The article is organized as follows. In Sec. II we give a brief account of how tunneling rates in dissipative quantum systems are calculated within the $\text{Im}F$ approach. Then, for the generic case of a cubic potential the two

*Electronic address: mduck@tfp1.uni-freiburg.de

models of low frequency environments are analysed, a sluggish bath model in Sec. III, and a model that incorporates additional dynamical modes with a $1/f$ characteristic in Sec. IV. The MQT readout in the quantonium device is addressed in Sec. V, particularly the Zener flip MQT. At the end some conclusions are given.

II. FREE ENERGY METHOD FOR TUNNELING RATES

The stochastic motion of a one-dimensional degree of freedom q with mass M in a potential field $V(q)$ is determined by a classical Langevin equation

$$M\ddot{q} + M \int_0^t ds \gamma(t-s)\dot{q}(s) + \frac{\partial V}{\partial q} = \xi(t). \quad (1)$$

The damping kernel $\gamma(t)$ and the Gaussian fluctuating force with $\langle \xi(t) \rangle = 0$ are related by the fluctuation-dissipation theorem $\langle \xi(t)\xi(s) \rangle = Mk_B T \gamma(t-s)$. The situation where a particle is initially confined in a metastable well and, as time elapses, leaves it due to thermal activation has been studied in a variety of systems [6, 21]. In the low temperature range below a certain crossover temperature T_0 , however, quantum tunneling is known to be the dominant escape process. Particularly, for an undamped system one has $T_0 = \hbar\omega_0/(2\pi k_B)$ where ω_0 denotes the frequency for oscillations around the minimum of the well (plasma frequency).

To describe quantum barrier penetration in presence of a dissipative environment, one starts from a system+reservoir model $H = H_0 + H_B + H_I$, where

$$\begin{aligned} H_0 &= \frac{p^2}{2M} + V(q) \\ H_B &= \sum_i \frac{p_i^2}{2m_i} + \frac{1}{2} m_i \omega_i^2 x_i^2 \\ H_I &= -q \sum_i c_i x_i \end{aligned} \quad (2)$$

This model of a bath consisting of harmonic oscillators captures linear dissipation and equivalently mimics an environment with Gaussian statistics. In the limit of a quasi-continuum of oscillators the effective influence of the heat bath is determined by the temperature T and the spectral bath density $J(\omega)$. Classically, for this model one regains the Langevin equation (1) where the Laplace transform of the damping kernel

$$\hat{\gamma}(z) = \int_0^\infty dt \gamma(t) e^{-zt} \quad (3)$$

is related to the spectral density via

$$\hat{\gamma}(z) = \frac{1}{M} \int_0^\infty \frac{d\omega}{\pi} \frac{J(\omega)}{\omega} \frac{2z}{\omega^2 + z^2}. \quad (4)$$

To obtain the tunneling rate, the usual procedure is to apply the so-called Im- F method. It is based on the

calculation of the free energy $F = (-1/\beta) \log Z$ and thus of the partition function Z of an unstable system. Most conveniently, this is done within the path integral representation which gives, after tracing out the bath degrees of freedom exactly, the partition function of the reduced systems as

$$Z = \int_{q(-\hbar\beta/2)=q(\hbar\beta/2)} \mathcal{D}q e^{-S[q]/\hbar} \quad (5)$$

with the effective Euclidean action functional $S[q] = S_0[q] + S_I[q]$ where

$$S_0[q] = \int_{-\hbar\beta/2}^{\hbar\beta/2} d\tau \left[\frac{M}{2} \dot{q}^2 + V(q) \right] \quad (6)$$

represents the bare system and

$$S_I[q] = -\frac{1}{2} \int_{-\hbar\beta/2}^{\hbar\beta/2} d\tau \int_{-\hbar\beta/2}^{\hbar\beta/2} d\tau' K(\tau-\tau') q(\tau) q(\tau') \quad (7)$$

originates from the coupling to the heat bath (influence functional). The influence kernel follows from

$$K(\tau) = \int_0^\infty \frac{d\omega}{\pi} J(\omega) \frac{\cosh[\omega(\hbar\beta/2 - \tau)]}{\sinh(\omega\hbar\beta/2)} \quad (8)$$

and is directly related to the analytic continuation to imaginary times of the force-force autocorrelation function of the bath $L(t) = \langle \hat{\xi}(t)\hat{\xi}(0) \rangle$ where $\hat{\xi} = \sum_i c_i x_i$, i.e. $K(\tau) = L(-i\tau)/\hbar$. Further, due to the relation (4) the influence kernel can be inferred from the classical damping kernel [6, 22].

The above path integral (5) sums over all closed paths in the imaginary time interval $[-\hbar\beta/2, \hbar\beta/2]$. In case of sufficiently high potential barriers a semiclassical approximation applies so that the partition function is dominated by all periodic minimal action paths and Gaussian fluctuations around them. It turns out that while fluctuations around a well minimum of a metastable potential are stable, those around a barrier top are not. As shown by Langer [7], due to an analytic continuation this gives rise to an imaginary contribution to the partition function $Z \approx Z_w + iZ_b = Z_w(1 + iZ_b/Z_w)$ which, even though it is exponentially small compared to the well contribution Z_w , must be taken into account to finally obtain the escape rate [1, 7]

$$\Gamma = -\frac{2}{\hbar} \text{Im} F = \frac{2}{\hbar\beta} \frac{Z_b}{Z_w}. \quad (9)$$

For the non-dissipative case and $T = 0$ the method is completely equivalent to the WKB formalism and in other ranges its results have been verified by full dynamical approaches [23] (see also [8]). Its theoretical predictions have been thoroughly tested in comparison with experimental data over broad temperatures ranges and for various systems [6]. The advantage of the method is that it enables us to calculate the decay rate of a metastable

system from a purely thermodynamic quantity without considering the complicated real time dynamics.

The archetypical form of a metastable potential is

$$V(q) = \frac{M}{2} \omega_0^2 q^2 \left(1 - \frac{q}{q_0}\right) \quad (10)$$

with a well located around $q = 0$ and a barrier top at $q_b = 2q_0/3$. The barrier height is $V_b = 2/27 M \omega_0^2 q_0^2$ and the well frequency ω_0 . Metastability justifying a semi-classical approximation to the partition function then means that $V_b \gg \hbar \omega_0, k_B T$. For a current-biased Josephson junction the known tilted washboard potential for its phase takes locally the above form of a cubic surface.

Accordingly, in the low temperature domain Z_b is dominated by the so-called bounce orbit, a minimal action path that runs in the time interval $[-\hbar\beta/2, \hbar\beta/2]$ through the inverted barrier potential $-V(q)$ with minimal action S_b . The corresponding tunneling rate turns out to be

$$\Gamma = \sqrt{\frac{S_b}{2\pi\hbar}} \sqrt{\frac{D_0}{D'_1}} e^{-S_b/\hbar} \quad (11)$$

where D_0 and D'_1 are functional determinants capturing Gaussian fluctuations around the constant well orbit $q(\tau) = 0$ and the bounce, respectively. In the latter one, the contribution from a zero mode direction in function space is omitted. In absence of a heat bath and for $T = 0$ the above expression leads to

$$\Gamma_0 = 6\omega_0 \sqrt{\frac{6v}{\pi}} e^{-36v/5} \quad (12)$$

where

$$v = \frac{V_b}{\hbar\omega_0} \quad (13)$$

is the dimensionless barrier height.

III. SLUGGISH BATH

While the impact of moderate to fast noise on tunneling rates has been elucidated analytically and numerically in the past [6], here, we focus on the low frequency limit and start with a sluggish bath. This means that the fastest modes available in the environment are still slow on the thermal time scale and compared to the system's well frequency. Specifically, we assume a spectral density $J_{<}(\omega)$ with a cut-off frequency ω_c , i.e. $J_{<}(\omega) = 0$, for $\omega > \omega_c$, obeying $\hbar\beta\omega_c \ll 1$ and $\omega_c/\omega_0 \ll 1$. As a consequence, the influence kernel becomes approximately constant

$$K(\tau) \approx \frac{2}{\hbar\beta} \int_0^\infty \frac{d\omega}{\pi} \frac{J_{<}(\omega)}{\omega} \equiv \frac{2}{\hbar\beta} J_s, \quad (14)$$

and the influence functional simply reads

$$S_I[q] \approx \frac{-J_s}{\hbar\beta} \left[\int_{-\hbar\beta/2}^{\hbar\beta/2} d\tau q(\tau) \right]^2. \quad (15)$$

Any bath coupling establishes correlations with corresponding memory times that relate the time evolution of the system at the present with its past. The time independent influence kernel of (15) can be understood as the limiting case where the frequencies of the environmental degrees of freedom are so low, that the critical correlation time ranges over the whole interval $[-\hbar\beta/2, \hbar\beta/2]$.

The sluggish bath can now most conveniently be treated by exploiting a Hubbard-Stratonovich transformation and introducing an auxiliary variable. Accordingly, the partition function is obtained as

$$Z(\sigma_x) = \sqrt{\frac{1}{2\pi\sigma_x}} \int_{-\infty}^{\infty} dx \exp\left(-\frac{x^2}{2\sigma_x}\right) Z(x), \quad (16)$$

where $Z(x)$ is the path integral

$$Z(x) = \int \mathcal{D}q e^{-S_x[q]/\hbar}. \quad (17)$$

The action functional $S_x[q] = S_0[q] + S_{x,I}[q]$ with

$$S_{x,I}[q] = x \int_{-\hbar\beta/2}^{\hbar\beta/2} d\tau q(\tau) \quad (18)$$

can be seen as a linear coupling between the "centroid" of the imaginary time orbit and a constant "external force". The total partition function is thus represented as an average over individual partition functions where the contribution of each one is weighted according to a Gaussian distribution with width $\sigma_x = 2J_s/\beta$.

Now, by a proper coordinate shift for a fixed value of the auxiliary variable $q = \tilde{q} + Q(x)$, the $S_{x,I}$ contribution in the effective action is absorbed in a potential contribution of an effective bare system. While the measure of the path integral remains unchanged, the parameters of the shifted potential become x -dependent, namely,

$$\tilde{V}(q, x) = \frac{M}{2} \tilde{\omega}_0(x)^2 q^2 \left(1 - \frac{q}{\tilde{q}_0(x)}\right), \quad (19)$$

where \tilde{q} and $\tilde{\omega}_0$ are defined by demanding that $xq + V(q) = \tilde{V}(\tilde{q}, x) + V(Q(x)) + xQ(x)$. With the abbreviation

$$\alpha(x) = \sqrt{1 + \frac{6x}{M\omega_0^2 q_0}} \quad (20)$$

one obtains the coordinate shift and the modified parameters as

$$Q(x) = \frac{q_0}{3} [1 - \alpha(x)] \quad (21)$$

$$\tilde{\omega}_0(x) = \omega_0 \sqrt{\alpha(x)} \quad (22)$$

$$\tilde{q}_0(x) = q_0 \alpha(x). \quad (23)$$

The partition function for fixed x now takes the form

$$Z(x) = e^{-\beta[V(Q(x)) + xQ(x)]} \oint \mathcal{D}\tilde{q} e^{-\frac{1}{\hbar} \tilde{S}_0[\tilde{q}; x]}, \quad (24)$$

where $\tilde{S}_0[\tilde{q}; x]$ denotes the action of the bare system (6) with the x dependent potential \tilde{V} from (19).

Now, in line with the semiclassical approximation, for sufficiently small width σ_x (details see below) the average over the auxiliary variable can be treated together with the fluctuations around the bounce $\tilde{q} = \tilde{q}_B + \delta\tilde{q}$ in steepest decent approximation : The full action is expanded around the bounce q_b for $x = 0$ up to terms of second order. This results in

$$\begin{aligned} \tilde{S}_0[\tilde{q}; x] = & S_b(x=0) + 4\frac{q_0}{\omega_0}x + \frac{3}{M\omega_0^3}x^2 \\ & + \frac{1}{2} \int_{-\hbar\beta/2}^{\hbar\beta/2} d\tau \delta\tilde{q} \frac{M}{2} \left(-\partial_\tau^2 + \frac{\tilde{V}''(\tilde{q}_B, x=0)}{M} \right) \delta\tilde{q} \\ & + O(x^3, \delta\tilde{q}^3). \end{aligned} \quad (25)$$

where S_b is the minimal action corresponding to q_b . In this second order approximation the last term in (26) is independent of x and the remaining path integral over the fluctuations yields the known functional determinant for $x = 0$. The total rate then factorizes: The $x = 0$ -part coincides with the non-dissipative tunneling rate $\Gamma(\beta)$ in a cubic potential; the remaining x -dependent terms in (26) enter into the average over the Gaussian distribution. Accordingly, the total rate reads

$$\Gamma_s(j, \theta) = \Gamma(\theta) I_s(j, \theta), \quad (26)$$

where we introduced dimensionless quantities $\theta = 2\pi/(\omega_0\hbar\beta)$ and $j = 2J_s/(M\omega_0^2)$, and the correction factor

$$I_s(j, \theta) = \sqrt{\frac{1-j}{1-j+\frac{6j\theta}{2\pi}}} \exp \left[\frac{108\frac{j\theta}{2\pi}v}{(1-j+\frac{6j\theta}{2\pi})} \right]. \quad (27)$$

The correction factor provides a restriction on σ_x which in turn defines the range where the steepest descent approximation for the x -average is justified. From $j - 6j\theta/2\pi \ll 1$ one finds

$$\frac{J_s}{M\omega_0^2} \ll 1. \quad (28)$$

For example, in case of low frequency Drude friction $J_<(\omega) = M\gamma\omega\omega_c^2/(\omega^2 + \omega_c^2)$ this leads to $\gamma\omega_c/\omega_0^2 \ll 2$ which due to $\omega_c/\omega_0 \ll 1$ allows even for stronger friction. Upon further inspection, one sees that sufficiently below the crossover temperature $\theta \ll 1$ the full rate (26) displays a dominating linear temperature increase due to its correction factor, while the bare rate approaches its zero temperature limit Γ_0 (12) since deviations become exponentially small in $2\pi/\theta$. This linear enhancement in T is a specific feature of a sluggish bath $\omega_c\hbar\beta \ll 1$. We note that thus in (27) the limit $T \rightarrow 0$ cannot be performed for fixed ω_c , but must include also $\omega_c \rightarrow 0$. Accordingly, zero-point fluctuations of the bath modes, which lead to the well-known counter term and renormalize the bare potential [6, 11], do not appear here.

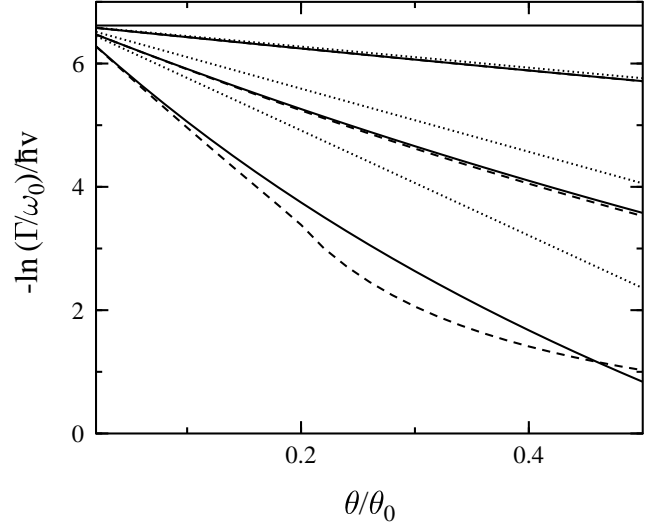


FIG. 1: MQT rates in presence of a sluggish bath vs. temperature for various values of the coupling constant $j = 0.0, 0.1, 0.3, 0.5$ (from top to bottom). Shown are results according to (26) (solid), numerical results (dashed) and perturbative results according to (29) (dotted).

An alternative procedure to calculate the tunneling in the limit of very weak dissipation and temperatures $T \ll T_0$ relies on a perturbative treatment around the non-dissipative bounce for $T = 0$. The first order correction to the bare bounce action S_b is determined by the influence functional $S_I[q]$ in (15) evaluated along the $T = 0$ -bounce q_b . Here, we obtain

$$S_I[q_b]/\hbar = -108 \frac{j\theta v}{2\pi} \quad (29)$$

in accordance with the result obtained above in (26) up to terms linear in j . Hence, the expression (27) applies also to larger values for j beyond the validity of the first order perturbation theory (see below). In this context we mention that the same result can be obtained by considering fluctuations in a control parameter of the rate, e.g. the external bias current for Josephson junctions, and then taking the average over the change of the dominant exponential factor with an appropriate Gaussian distribution [11].

In order to illustrate the accuracy of the expression (26), we evaluated the rate numerically according to the general formula (11) in the case of weaker dissipation and a sluggish bath (see fig. 1). The bounce is gained from its Fourier coefficients $q_b(\tau) = \sum Q_n \exp(i\nu_n\tau)$ according to the equation of motion in the inverted potential (see [9] for details). For the comparison, we further approximated $\Gamma(\theta) \approx \Gamma(0)$ in (26) which is correct up to exponentially small corrections for low temperatures. The agreement with the analytical result is excellent even for $j = 0.5$ and sufficiently low temperatures, while the perturbative result displays negligible deviations from the numerical data only for $j \leq 0.1$. Obviously, the dissipa-

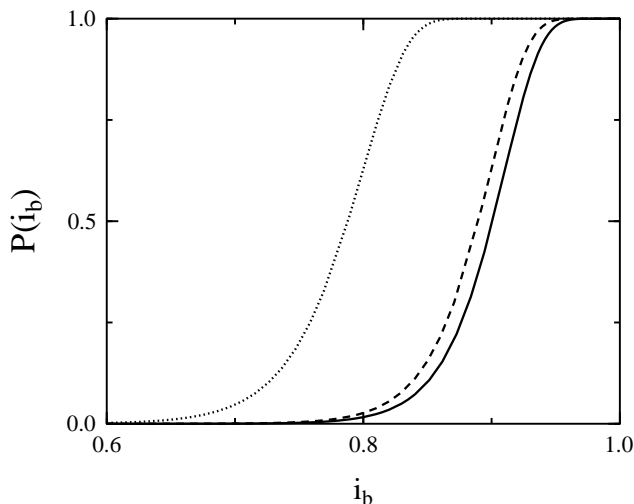


FIG. 2: Probability for escape vs. bias current for a Josephson junction with dimensionless barrier height $v = 3$ and various values of the coupling to a sluggish bath $j = 0.0$ (solid), 0.1 (dashed), 0.3 (dotted).

tive rate is always enhanced roughly linearly compared to the bare one due to the impact of the sluggish bath fluctuations.

In experiments on Josephson junction circuits typically the escape rate is not measured directly, but rather the probability for escape as the height i_b of an external bias current pulse varies, while keeping the width Δt in time of the pulse constant, i.e.,

$$P(i_b) = 1 - e^{-\Gamma(i_b) \Delta t}. \quad (30)$$

The parameters of the cubic potential (10) depend for i_b close to the critical current i_0 of the junction on the bias current via $\omega(i_b) = \omega(i_b = 0)[1 - (i_b/i_0)^2]^{1/4}$ and $V_b(i_b) = V_b(i_b = 0)(1 - i_b/i_0)^{3/2}$. In fig. 2 the corresponding "s-curves" are depicted for various strengths of the coupling. Since in presence of slow bath modes the rate is larger than the bare one, the s-curves are shifted towards smaller values of the bias current and exhibit a smaller slope.

IV. SLUGGISH BATH AND $1/f$ -DAMPING

Having analyzed the influence of the coupling to sluggish bath modes we now turn to the case where in addition to a pronounced low frequency part a tail of slow to moderate frequency modes are present. In particular, we consider dynamical fluctuations the power spectrum of which display a $1/f$ characteristic.

A. Spectral density and influence kernel

In present experiments on superconducting qubits $1/f$ noise has been found to be the most dominant (and most

annoying) source of noise [18]. While in principle one could start with a truly microscopic model as in [12, 24], here, we proceed with a somewhat simplified procedure and effectively mimic the $1/f$ noise by a proper spectral density of a heat bath. We write

$$J(\omega) = J_<(\omega) + J_{1/f}(\omega) \quad (31)$$

where $J_<$ with $J_<(\omega) = 0$ for $\omega > \omega_c$ comprises all sluggish environmental modes and $J_{1/f}$ with $J_{1/f}(\omega) = 0$ for $\omega < \omega_-$ and $\omega > \omega_+$ contains its dynamical modes. For convenience, we introduced here in addition to ω_c the lower cut-off ω_- with $\omega_c \leq \omega_-$ to have better control over the two domains of the spectrum. Clearly, the separation into a sluggish part and a dynamical one is somewhat arbitrary and depends on the specific experimental situation, i.e. on the relevant time scales involved and the measurement protocol imposed. We will see at the end, however, that our main findings are independent of these latter cut-off frequencies as long as they lie in a range $\omega_c, \omega_- \ll \omega_0$. The upper cut-off ω_+ is taken to be only somewhat smaller than ω_0 such that $2\pi/\omega_+ \hbar \beta$ is still sufficiently larger than 1. For instance, for typical experimental values $\omega_0 \simeq 50$ GHz and $T \simeq 20$ mK corresponding to $\omega_0 \hbar \beta \approx 20$, one may assume ω_+ to lie in the GHz range as well, i.e. $\omega_+ \simeq 1$ GHz, leading to $2\pi/\omega_+ \hbar \beta \approx 15$.

Now, the power spectrum of bath fluctuations follows from the symmetrized force-force auto-correlation function of $\hat{\xi} = \sum c_\alpha x_\alpha$ as

$$\tilde{S}_\xi(\omega) = \frac{1}{2\pi} \int_{-\infty}^{+\infty} e^{i\omega t} \langle \hat{\xi}(t) \hat{\xi}(0) \rangle_\beta dt. \quad (32)$$

Experimentally, background charge fluctuations in mesoscopic circuits have shown to give rise to a behavior $\tilde{S}_\xi(\omega) = s_0/\omega$ over a broad frequency range ($1/f$ noise). According to (31) the spectral density $J_{1/f}$ of the *dynamical* modes can then be calculated using the fluctuation-dissipation-theorem

$$\frac{s_0}{\omega} \Theta(\omega - \omega_-) \Theta(\omega_+ - \omega) = \hbar \coth(\omega \hbar \beta) J_{1/f}(\omega). \quad (33)$$

As a consequence of (31) the influence kernel $K(\tau)$ splits into two contributions where the usual procedure is to split off from the second one a part local in time, i.e.,

$$K(\tau) = \frac{2J_s}{\hbar\beta} - k(\tau) + J_f : \delta(\tau) : \quad (34)$$

where

$$J_f = \int_0^\infty \frac{d\omega}{\pi} \frac{2J_{1/f}(\omega)}{\omega} \quad (35)$$

and

$$k(\tau) = \frac{M}{\hbar\beta} \sum_{n=-\infty}^{\infty} |\nu_n| \hat{\gamma}(|\nu_n|) e^{i\nu_n \tau}. \quad (36)$$

Here, $:\delta(\tau):$ is the periodically continued δ function with period $\hbar\beta$ and $\nu_n = 2\pi n/\hbar\beta$ denote the Matsubara frequencies.

The Fourier coefficients of the dynamical part of the influence kernel are obtained from the spectral density via the relation (3). This way, for a spectral density with dynamical modes one finds from (33) $J_{1/f}(\omega) = \kappa_{1/f}(\omega) M \Theta(\omega - \omega_-) \Theta(\omega_+ - \omega)$ where in the relevant frequency domain $\kappa_{1/f}(\omega) = s_0 \tanh(\omega \hbar\beta)/(\hbar\omega M) \approx \kappa$ is basically constant in frequency and taken to be independent of temperature as well. Consequently, the amplitude of the power spectrum s_0 increases linearly with temperature T in agreement with an electron trapping mechanism for $1/f$ noise [17]. Eventually, one arrives at

$$\hat{\gamma}(|\nu_n|) = \frac{\kappa}{|\nu_n|\pi} \log \left(\frac{1 + \nu_n^2/\omega_-^2}{1 + \nu_n^2/\omega_+^2} \right). \quad (37)$$

In particular, $|\nu_n|\hat{\gamma}(|\nu_n|) = 0$ for $n = 0$, while for $n \neq 0$ due to $\nu_n/\omega_- \gg \nu_n/\omega_+ \gg 1$ one expands $|\nu_n|\hat{\gamma}(|\nu_n|) \approx (2\kappa/\pi) \log(\omega_+/\omega_-) - (\kappa/\pi)(\omega_+^2 - \omega_-^2)/\nu_n^2$. The constant factor $(2\kappa/\pi) \log(\omega_+/\omega_-)$ leads in the time domain to a contribution proportional to $[\delta(\tau) : -1/\hbar\beta]$ where the part containing the δ function exactly cancels in (34) the contribution proportional to J_f . In turn, this means that a spectral density corresponding to $1/f$ noise does *not* generate a contribution in the influence functional local in time and renormalizing the potential.

Now, the influence functional (7) takes the form

$$S_I[q] = -\frac{\tilde{J}_s}{\hbar\beta} \left(\int_{-\hbar\beta/2}^{\hbar\beta/2} d\tau q(\tau) \right)^2 + \frac{1}{2} \int_{-\hbar\beta/2}^{\hbar\beta/2} d\tau \int_{-\hbar\beta/2}^{\hbar\beta/2} d\tau' q(\tau) \tilde{k}(\tau - \tau') q(\tau') \quad (38)$$

with

$$\tilde{J}_s = J_s + (M\kappa/\pi) \log(\omega_+/\omega_-) \quad (39)$$

being an effective sluggish bath coupling and a non-local damping kernel

$$\tilde{k}(\tau) = \zeta \frac{M}{\hbar\beta} \sum'_{n=-\infty}^{\infty} \frac{1}{\nu_n^2} e^{i\nu_n\tau}, \quad (40)$$

where in the sum the $n = 0$ term is omitted and

$$\zeta = \kappa(\omega_+^2 - \omega_-^2)/\pi \approx \kappa\omega_+^2/\pi. \quad (41)$$

In fact, the above Fourier series can be summed up exactly and yields $\tilde{k}(\tau) = \sum_{l=-\infty}^{\infty} \tilde{k}_l(\tau)$ with

$$\tilde{k}_l(\tau) = \frac{M\zeta}{2\hbar\beta} \left[\tau - (2l+1)\frac{\hbar\beta}{2} \right]^2 - \frac{M\zeta\hbar\beta}{24} \quad \text{for } \tau \in (l\hbar\beta, (l+1)\hbar\beta). \quad (42)$$

This way, the influence of the sluggish modes is described by one effective parameter \tilde{J}_s independent of the specific cut-off frequencies ω_c and ω_- , and the only relevant frequency scale of the bath is ω_+ .

B. Tunneling rate

With the influence kernel at hand, the tunneling rate can now be determined. The sluggish modes leading to the static contribution in (39) are treated analogous to the procedure described in the previous Sect. III. Note that the corresponding constant coordinate shift does not change the form of the dynamical part since $\int_0^{\hbar\beta} d\tau \tilde{k}(\tau) = 0$. The effective action is obtained as $\tilde{S}[\tilde{q}; x] = \tilde{S}_0[\tilde{q}; x] + \tilde{S}_I[\tilde{q}]$ with

$$\tilde{S}_I[q] = \frac{1}{2} \int_{-\hbar\beta/2}^{\hbar\beta/2} d\tau \int_{-\hbar\beta/2}^{\hbar\beta/2} d\tau' \tilde{k}(\tau - \tau') \tilde{q}(\tau) \tilde{q}(\tau') \quad (43)$$

with the x -dependent potential given in (19).

For the case of weak dissipation and low temperatures damping due to dynamical modes is treated perturbatively to first order in the dimensionless coupling $\tilde{\kappa} = \kappa/\omega_0^2$ by substituting the undamped $T = 0$ -bounce into the influence functional S_I . Clearly, due to the x -dependence of the bare action, this orbit becomes also x -dependent and reads

$$\tilde{q}_{b,x}(\tau) = \frac{\tilde{q}_0(x)}{\cosh^2(\tilde{\omega}_0(x)\tau/2)}. \quad (44)$$

Then, for the total partition function one arrives at

$$Z(\sigma_x, \alpha, \beta) = \sqrt{\frac{1}{2\pi\sigma_x}} \int_{-\infty}^{\infty} dx e^{-\frac{x^2}{2\sigma_x}} \times e^{-\frac{1}{\hbar} S_{1/f, \text{dyn}}(x)} Z(x), \quad (45)$$

where $Z(x)$ is specified in (24) and $S_{1/f, \text{dyn}}(x) = \tilde{S}_I[\tilde{q}_{b,x}]$. Again the x -integration can be carried out by expanding the exponent up to second order in x . The resulting rate expression is given by

$$\Gamma_{s,1/f}(\tilde{j}, \tilde{\kappa}, \theta) = \Gamma(\theta) I_{s,1/f}(\tilde{j}, \tilde{\kappa}, \theta) \quad (46)$$

with the dimensionless temperature $\theta = 2\pi/\omega_0\hbar\beta$ and the dimensionless couplings $\tilde{j} = 2\tilde{J}_s/M\omega_0^2$ and $\tilde{\kappa} = \kappa/\omega_0^2$. The correction factor is now obtained as

$$I_{s,1/f}(\tilde{j}, \tilde{\kappa}, \theta) = \sqrt{\frac{1 - \tilde{j}}{1 - \tilde{j} + 6\tilde{j}\theta/2\pi}} \exp[-S_{1/f, \text{dyn}}(0)/\hbar] \times \exp\left[\frac{27\theta\tilde{j}v}{\pi} \frac{2 + \omega_0 S'_{1/f, \text{dyn}}(0)/q_0}{1 - \tilde{j} + 6\tilde{j}\theta/2\pi}\right]. \quad (47)$$

Here $S'_{1/f, \text{dyn}}$ denotes the derivative of the damping term with respect to x and is of first order in $\tilde{\kappa}$ as well as $S_{1/f, \text{dyn}}$. Apparently, the influence of the environment leads to two competing effects: The static modes give rise to a rate enhancement, while the contribution of the dynamical ones depresses the rate. To get further insight, we thus evaluate the action $S_{1/f, \text{dyn}}(0)$ analytically by exploiting the results in (43) and (44), and obtain

$$S_{1/f, \text{dyn}}(0)/\hbar = \frac{M\tilde{\kappa}q_0^2\omega_+^2}{\pi\hbar\omega_0} \left(\frac{a_1}{\omega_0\hbar\beta} - 2a_2 + \frac{2\omega_0\hbar\beta}{3} \right) \quad (48)$$

with constants $a_1 = 26.319\dots, a_2 = 4.00\dots$. In the low temperature range $\omega_0 \hbar \beta \gg 1$ this reduces to

$$S_{1/f,\text{dyn}}(0)/\hbar \approx v \frac{9\tilde{\kappa}}{\pi} \frac{\omega_+}{\omega_0} \omega_+ \hbar \beta \quad (49)$$

where we used (41). An analogue calculation for the derivative of the damping term yields

$$S'_{1/f,\text{dyn}}(0) \approx \frac{6}{M\omega_0^2 q_0} S_{1/f,\text{dyn}}(0) - \frac{3}{M\omega_0^2 q_0} \frac{27\hbar v \tilde{\kappa} \omega_+^2}{2\pi \omega_0^2} \left(\frac{b_1}{\omega_0 \hbar \beta} - 2b_2 + \frac{\omega_0 \hbar \beta}{3} b_3 \right) \quad (50)$$

with the constants $b_1 = 52.6379\dots, b_2 = 6.00$ and $b_3 = 2.00$.

We can now compare the leading order terms in the two exponents of the correction factor (47). With respect to the static part, it is sufficient to consider only the dominant term $54\theta\tilde{j}v/\pi$ and there to focus on the contribution stemming from $J_{1/f}$, namely, $S_{1/f,\text{stat}} = 108\theta v \kappa \log(\omega_+/\omega_-)/(\pi^2 \omega_0^2)$. Accordingly,

$$\frac{S_{1/f,\text{stat}}}{S_{1/f,\text{dyn}}} = \frac{48 \log(\omega_+/\omega_-)}{(\omega_+ \hbar \beta)^2} \gg 1, \quad (51)$$

which reveals that the dynamical contribution of the environment is basically negligible compared to the static one. Hence, the system-bath coupling parameters obey the relation $\tilde{j}/\tilde{\kappa} \gg 2(\omega_+ \hbar \beta / 2\pi)^2$. For the tunneling process a low to moderate frequency bath with a $1/f$ characteristic can thus be treated as static and always leads to a rate enhancement which roughly grows linearly with temperature. The physical reason for this is simply that the environment has only a time period of the order of $1/\omega_0$ to probe the system while tunneling. On this time scale the dominant part of the bath modes is basically frozen, while the contribution of the dynamical ones remains small for a $1/f$ spectrum. A changeover from a short to a long time behavior cannot be observed in contrast to the decay of coherent superpositions in superconducting qubits [13, 14, 15, 16].

In order to illustrate these findings we show in fig. 3 the ratio $\Gamma_{s,1/f}(\theta)/\Gamma_0$ for varying temperature and different damping strength $\tilde{j} = \tilde{\kappa}$. The analytical expression obtained in (46) coincides within this range with the numerical data. As seen in the inset, the influence of the dynamical modes to suppress the MQT rate is very small and only increases slightly at very low temperatures. Note again, that for fixed ω_c the limit $T \rightarrow 0$ cannot be reached. Typical temperatures in experiments, however, lie in the range about 20 mK corresponding to $\theta/\theta_0 \simeq 0.1 \dots 0.3$.

V. QUANTRONIUM QUBIT

The "quantronium" is a solid state based qubit setup consisting of a Cooper pair box whose Josephson junction is split in two small junctions with Josephson energy

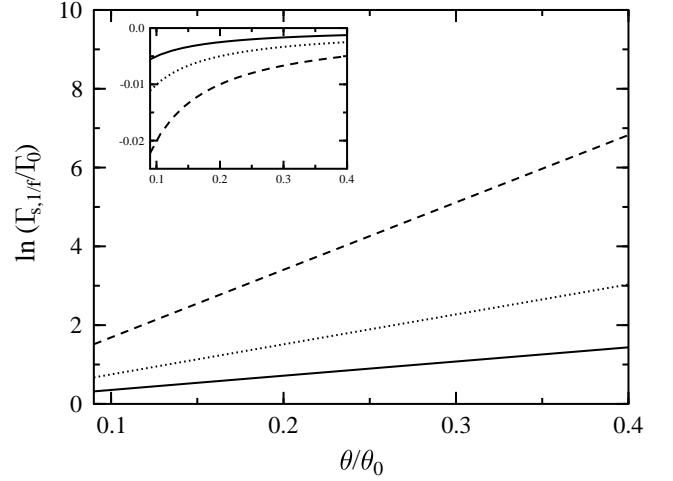


FIG. 3: Rate enhancement due to a sluggish bath with $1/f$ noise vs. temperature. The couplings constants are $\tilde{j} = \tilde{\kappa} = 0.05$ (solid), 0.1 (dotted), 0.2 (dashed), and $\omega_+/\omega_0 = 1/50$. The inset shows the suppression only due to dynamical modes ($\tilde{j} = 0$), but with the same values for $\tilde{\kappa}$

E_J , delimiting an island with capacitance C and charging energy $E_C = (2e)^2/2C$ [4]. The two lowest lying states of the box with energies E_0 and E_1 encode a qubit and in the circuit give rise to loop currents of opposite direction. In parallel with the box is a third big Josephson junction (with $E'_J \gg E_J$ and $E'_C \ll E_C$) which serves as a detector. For the read-out this big junction is biased by an external current pulse so that the total bias current seen by the junction depends on the state of the qubit. The measurement consists of adiabatically driving the big junction into the regime where MQT sets in. Due to the exponential sensitivity of the tunneling rate on the total bias current, the two qubits states can efficiently be discriminated. In the quantronium two dominant sources of noise influence the qubit, namely, charge noise and phase noise. The latter one is mainly due to noise in the big read-out junction and there, originates e.g. from fluctuations of the external bias current. In the sequel, we are interested in this low frequency noise affecting the phase of the big junction during the tunneling process.

The analysis of the device becomes particularly transparent in the charging regime ($E_C \gg E_J$) where the two qubit states are determined by superpositions of zero or one excess Cooper pairs on the island. Then, the Hamiltonian of the box-subsystem can be written in terms of Pauli matrices and by measuring all energies in units of E'_J the total dimensionless Hamiltonian of the circuit reads

$$h = e_C \sigma_z - e_J \cos\left(\frac{\theta + \phi}{2}\right) \sigma_x + \frac{P_\theta^2}{2M} - \cos(\theta) - i_b \theta \quad (52)$$

with the dimensionless parameters $e_C = (E_C/E'_J)(N_g - 1/2)$, $e_J = E_J/E'_J$, and $i_b = \hbar I_b / 2e E'_J$. Here, N_g is the reduced gate charge and I_b denotes the external bias current. ϕ represents the reduced magnetic

flux in units of $\hbar/2e$ and $M = C'E_J/4e^2$ is the mass of the artificial particle of the read-out junction with momentum P and conjugate phase θ the dynamics of which takes place in a tilted washboard potential $-\cos(\theta) - i_b\theta$. For further details we refer to [4, 19]. Due to the coupling between the two subsystems, the qubit and the big junction, the dynamics of θ can be seen as that of a particle with two internal states.

Now, we consider the situation when the qubit is initially ($i_b = 0$) prepared in its ground state. By rising the bias current $i_b > 0$ adiabatically the phase θ can be seen as a classical variable with negligible kinetic energy due to the large capacitance C' . Depending on the spin state, the artificial particle then evolves on adiabatic potential surfaces $\lambda_{\pm}(\theta)$ obtained by simply diagonalizing h in spin space for $M \rightarrow \infty$ [19]. When i_b is close to 1, however, the particle may tunnel out of the potential well. In this case the Hamiltonian is most conveniently represented in the spin basis at the minimum θ_{\min} of the lower surface $\lambda_{-}(\theta)$, i.e.,

$$H = \begin{pmatrix} \frac{p_{\theta}^2}{2M} + V_{+}(\theta) & \Delta(\theta) \\ \Delta(\theta) & \frac{p_{\theta}^2}{2M} + V_{-}(\theta) \end{pmatrix} \quad (53)$$

Here, the diabatic potential surfaces read

$$V_{\pm} = -\cos(\theta) - i_b\theta \pm \left(\sqrt{e_C^2 + V_0^2} + \frac{V_0[V(\theta) - V_0]}{\sqrt{e_C^2 + V_0^2}} \right) \quad (54)$$

and the off diagonal elements

$$\Delta(\theta) = \frac{e_C[V_0 - V(\theta)]}{\sqrt{e_C^2 + V_0^2}} \quad (55)$$

where $V(\theta) = e_J \cos(\frac{\theta+\phi}{2})$ and $V_0 = V(\theta_{\min})$. By construction, for $\theta = \theta_{\min}$ the off-diagonal elements vanish. Further, one approximates these diabatic surfaces in the well-barrier range by a cubic expansion around the well minimum θ_{\min}

$$V_{\pm}(q) = \frac{M\Omega_{\pm}^2}{2} (q - q_{\pm})^2 [1 - (q - q_{\pm})/q_{0,\pm}] + \delta_{\pm,+} \Delta V_{\min}, \quad (56)$$

where $q = \theta - \theta_{\min}$ is measured relatively to the minimum, $\delta_{\mu,\nu}$ denotes the Kronecker symbol, and $\Delta V_{\min} = V_{+}(\theta_{\min}) - V_{-}(\theta_{\min})$.

Now, as long as V_{\pm} are sufficiently separated from each other everywhere in the barrier range, i.e. $|V_{-} - V_{+}| \gg \Delta$, the spin degree of freedom is essentially frozen and the particle escapes through V_{-} via standard MQT (see fig. 4, left). The influence of noise for this scenario is thus captured by the findings of the previous sections.

There is an additional domain, however, which gives rise to an interesting MQT phenomenon [19, 20]. Namely, when the two diabatic surfaces cross each other in the barrier range (see fig. 4, right), the particle's spin may flip during the tunneling since this may enhance the probability for escape substantially. The standard MQT approach has then to be extended to include spin flips so

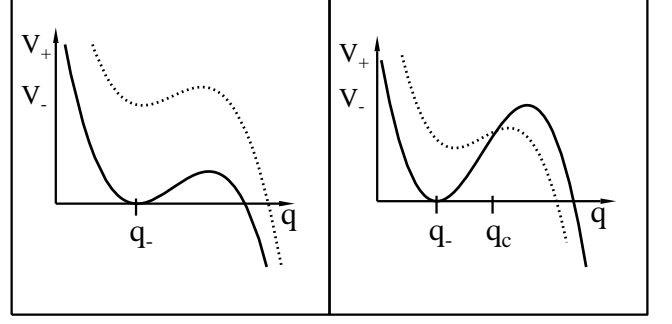


FIG. 4: Diabatic potential surfaces V_{+} (dashed) and V_{-} (solid) outside (left) and inside (right) the range where Zener flip tunneling occurs.

that the tunneling rate follows, in case of vanishing dissipation, from the imaginary part of the partition function

$$Z = \int \mathcal{D}q e^{-S_{-}[q]} \left\{ 1 + \sum_{n=1}^{\infty} \int_{-\hbar\beta/2}^{\hbar\beta/2} d\tau_{2n} \cdots \int_{-\hbar\beta/2}^{\tau_2} d\tau_1 \right. \\ \times \Delta(q(\tau_{2n})) \cdots \Delta(q(\tau_1)) \\ \times \left. \exp \left[\sum_{k=1}^n \int_{\tau_{2k-1}}^{\tau_{2k}} d\tau (V_{-}(q) - V_{+}(q)) \right] \right\}, \quad (57)$$

where S_{-} denotes the bare action on the surface V_{-} . The corresponding MQT rate can be cast into

$$\Gamma_{\text{tot}} = \Gamma_b + f_{\text{flip}}(\Delta_c) \exp(-S_{\text{flip}}/\hbar) \quad (58)$$

where Γ_b denotes the standard MQT rate without spin flip, while the second term captures contributions due to flips. The prefactor $f_{\text{flip}}(\Delta_c)$ with Δ_c the coupling at the crossing point of V_{\pm} is related to the probability for a spin flip to occur and S_{flip} is the action along the flip-bounce. It turns out that a theory based on the non-dissipative partition function (57) provides rates which are already in good agreement with experimental data [20]. Nevertheless, a deeper understanding of the impact of low frequency noise on the Zener-flip-tunneling is clearly needed.

It was found in [19] that when the particle traverses the intersection range of V_{\pm} sufficiently fast the flip contribution is dominated by two spin-flips. Further, in case of weak friction the most profound effect of dissipation on the rate is provided by the action factor. Hence, we focus on the two-flip bounce and its action at low temperatures. In generalization of (5), the dissipative flip-bounce action

takes the form

$$S_{\text{flip}}[q; s_1, s_2] = \int_{-\hbar\beta/2}^{\hbar\beta/2} d\tau \left\{ \frac{M}{2} \dot{q}^2 + V_-(q) + h_{s_1, s_2}(\tau) [V_+(q) - V_-(q)] \right\} - \frac{1}{2} \int_{-\hbar\beta/2}^{\hbar\beta/2} d\tau d\tau' q(\tau) K(\tau - \tau') q(\tau') \quad (59)$$

where h_{s_1, s_2} is the step function being unity in the interval $[s_1, s_2]$ and zero anywhere else and the kernel follows from (39). For the two flip contribution the action also depends on the flip times s_1 and s_2 . The influence kernel $K(\tau)$ gives according to the analysis of Sec. IV A rise to a static and a dynamical contribution, see (39). We first concentrate on weak friction for both, such that a perturbation theory to first order in \tilde{J}_s and $\tilde{\kappa}$ applies. By resorting again to a semiclassical evaluation this amounts to the fact to insert the undamped bounces q_b and q_{flip} , respectively, into the influence functional. The rate enhancement due to Zener flips can then be estimated by the difference between the simple bounce and the flip bounce actions, i.e.,

$$\Delta S(\tilde{J}_s, \tilde{\kappa}) = S_b(\tilde{J}_s = 0, \tilde{\kappa} = 0) - S_{\text{flip}}(\tilde{J}_s = 0, \tilde{\kappa} = 0) - \frac{\tilde{J}_s}{\hbar\beta} \left\{ \left[\int_{-\hbar\beta/2}^{\hbar\beta/2} d\tau q_b(\tau) \right]^2 - \left[\int_{-\hbar\beta/2}^{\hbar\beta/2} d\tau q_{\text{flip}}(\tau) \right]^2 \right\} + \frac{1}{2} \left\{ \int_{-\hbar\beta/2}^{\hbar\beta/2} d\tau d\tau' \tilde{\kappa}(\tau - \tau') [q_b(\tau)q_b(\tau') - q_{\text{flip}}(\tau)q_{\text{flip}}(\tau')] \right\}. \quad (60)$$

The explicit form for the flip bounce and its action has been given in [19] to which we refer for further details. Since the flip bounce always exhibits a smaller amplitude and width (see fig. 5), the terms in curly brackets are always positive. Hence, we arrive at the important result that weak static noise always lowers the rate enhancement due to Zener flip tunneling, while weak dynamical noise always increases its effect. The impact of which actually prevails depends only on the coupling strengths since the respective tunneling orbits enter both corrections in the same way. We note that so far (61) relies only on the weak coupling limit, but applies to any kind of spectral density of the environment.

As we have seen above, for a $1/f$ noise the impact of dynamical modes is much smaller than that of the sluggish ones so that we expect a shrinking of the enhancement. In order to see that explicitly, the tunneling orbits in presence of damping are determined numerically. Particularly, the flip-bounce is determined by a vanishing variation of $S[q; s_1, s_2]$ with respect to all periodic paths and their corresponding flip times. It turns out that the optimal spin flips occur just as the trajectory reaches the intersection point and that they are centered symmetrically around $\tau = 0$. For the stationary action the time

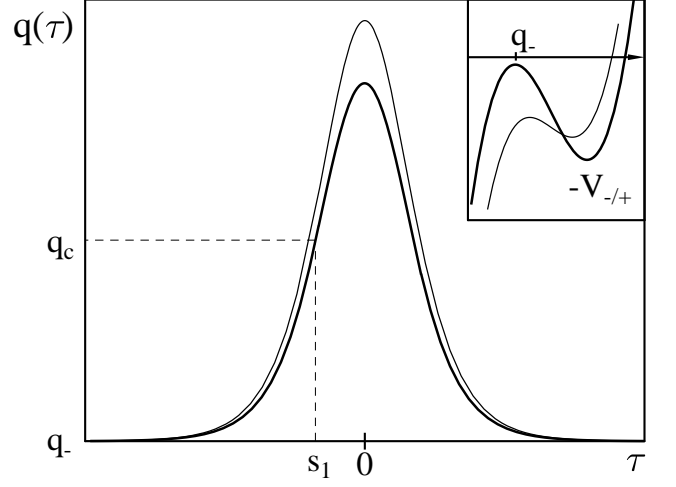


FIG. 5: Ordinary bounce (thin) and flip bounce trajectory (thick). The inset displays the inverted diabatic potentials (V_+ thin, V_- thick) intersecting at q_c .

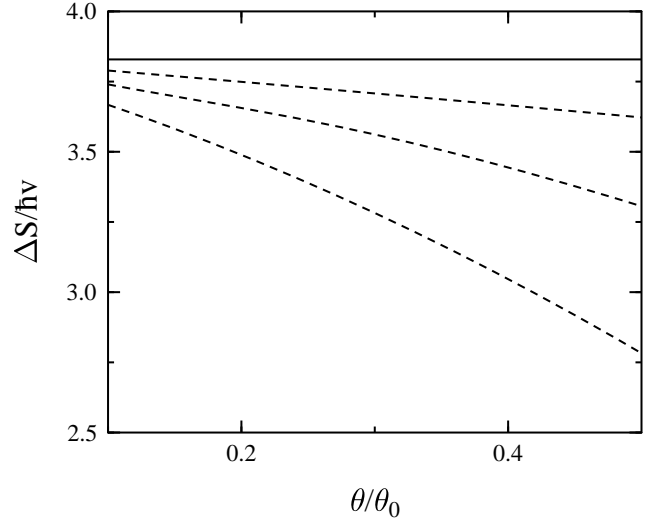


FIG. 6: Rate enhancement due to Zener flip tunneling vs. temperature in presence of a bath with a $1/f$ spectrum and various values for the coupling constant (from top to bottom) $\tilde{j} = 0.0$ (solid), $0.1, 0.2, 0.3$ (dashed).

dependent potential can therefore be replaced by a piecewise potential $V_c(q) = V_-(q)\Theta(q_c - q) + V_+(q)\Theta(q - q_c)$ where q_c denotes the intersection point. The equation of motion for the flip bounce thus reads

$$-M\ddot{q}_{\text{flip}}(\tau) + V'_c(q_{\text{flip}}) = \int_{-\hbar\beta/2}^{\hbar\beta/2} d\tau' K(\tau - \tau') q_{\text{flip}}(\tau'). \quad (61)$$

Unfortunately, the straightforward approach developed for standard MQT rates and exploited also in Sec. III, where the equation of motion is solved numerically by switching to Fourier space, does not work here due to the piecewise potential. Its derivative gives rise to

δ function contributions, which pose numerical instabilities that cannot be circumvented by the usual rescaling. We thus determined q_{flip} in coordinate space in an iterative procedure. One starts with the known flip-bounce for vanishing dissipation $q_{\text{flip}}^{(0)}$ on the right hand side and calculates the dissipative flip-bounce $q_{\text{flip}}^{(k)}$ by successively using $q_{\text{flip}}^{(k-1)}$ for the dissipative part. The final flip-bounce follows after a sufficient number of iterations and by preserving the boundary conditions $q_{\text{flip}}(\tau \rightarrow \infty) = 0$ for $\hbar\beta \rightarrow \infty$. Typically, convergence is achieved quickly after 5 – 10 steps depending on the dissipation strength. From the flip-bounce the corresponding action is obtained which, for weak friction, leads together with the non-dissipative prefactor $f_{\text{flip}}(\Delta_c)$ and the standard MQT rate to the total rate in the flip range.

In fig. 6 the rate enhancement due to Zener flip tunneling given by the action difference between standard bounce action and flip bounce action is shown for various values of the coupling to a $1/f$ bath. It is clearly seen that the impact of the static modes prevails and suppresses the enhancement with increasing temperature according to the above discussion. For weak coupling, however, the suppression remains small even at higher temperatures. To further illustrate the Zener flip effect on rate measurements, we show in fig. 7 the probability to escape $P(i_b)$ with varying bias current i_b [see (30)] for the quantonium circuit and in the range where Zener flips occur. Qualitatively, Zener flips lead to a pronounced shift of the s-curve towards smaller values of the external bias current, though, with a smaller slope in the first part of the curve. The influence of sluggish bath modes is to slightly move the Zener-curve back towards the standard MQT curve, but for weak damping this effect is hardly visible in the s-curves. By comparing with fig. 2, however, one realizes that the Zener-curve resembles a standard MQT curve in presence of a stronger low frequency environment. Experimentally, some further information about the influence of environmental modes is thus required to detect the Zener flip effect in a single s-curve measurement. The effect is clearly observable when one measures the bias current needed to maintain a certain value for $P(i_b)$ while sweeping through the Zener flip range by varying the magnetic flux ϕ [20].

VI. CONCLUSIONS

Macroscopic quantum tunneling has regained new interest in the context of quantum information processing based on Josephson junction circuits. In this paper we analyzed the influence of low to moderate frequency noise on the tunneling rate out of a metastable well, where the noise spectrum is restricted to frequencies somewhat smaller than the typical frequency for oscillations around the well bottom (plasma frequency). A sluggish bath leads to a rate enhancement linear in the temperature, in contrast to the typical T^2 behavior for ohmic environ-

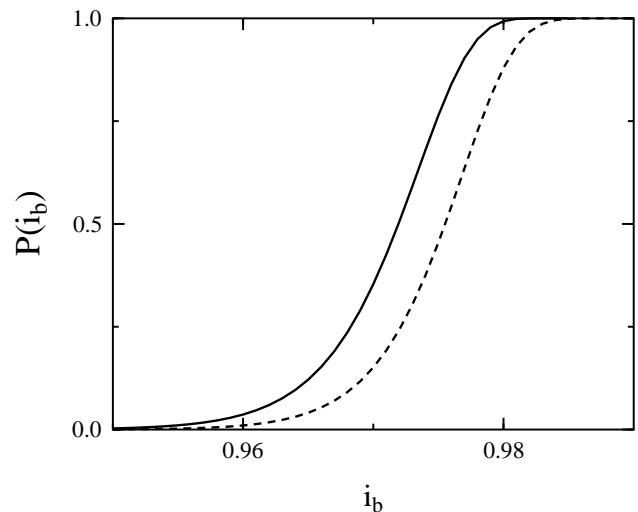


FIG. 7: Probability to escape vs. external bias current for the quantonium circuit and in the parameter range where Zener flip tunneling occurs. The solid line is the result including Zener flips, while the dashed one is generated using the standard MQT rate.

ments. For a sluggish bath with an additional $1/f$ characteristic it turns out that even in presence of dynamical modes the static component by far prevails. This verifies that for MQT processes $1/f$ noise can basically be treated as classical noise and in an adiabatic approximation where for very weak coupling one effectively averages over rates for an ensemble of potential barriers.

Based on these findings the impact of noise on a particular kind of MQT process has been studied, where a particle carrying a spin-1/2 as an internal degree of freedom experiences a Zener transition while tunneling. By comparing this new decay channel with ordinary MQT, we find that weak static noise suppresses the enhancement of Zener flip tunneling, while weak dynamical noise increases it. Further, we find that for escape probabilities (s-curves) the Zener flip effect leads qualitatively to a similar result as a standard MQT process under the stronger influence of sluggish bath modes. For the experimental observation of Zener flip tunneling it is thus advantageous to have an environment weakly coupled to the system (higher Q -factor) and a spectrum with a decreasing intensity towards low frequency modes, e.g. with a prevailing ohmic characteristic.

Acknowledgements

This work benefitted from fruitful discussions with E. Collin, D. Esteve, D. Vion, and H. Grabert. JA acknowledges a Heisenberg fellowship of the DFG.

[†] Present address: Department of Physics and Astronomy, University of Basel, Klingelbergstrasse 82, CH-4056

Basel, Switzerland

-
- [1] A.O. Caldeira, A.J. Leggett, Ann. Phys. (NY) **149**, 374 (1983).
 - [2] M.H. Devoret, D. Esteve, C. Urbina, J. M. Martinis, A. Cleland, and J. Clarke, in *Quantum Tunneling in Condensed Media*, Yu. Kagan and A.J. Leggett (eds.) (Elsevier, Amsterdam, 1992) and references therein.
 - [3] Y. Nakamura, Yu. A. Pashkin, and J.S. Tsai, Nature **398**, 786 (1999); J. M. Martinis, S. Nam, J. Aumentado, and C. Urbina, Phys. Rev. Lett **89**, 117901 (2002); I. Chiorescu, Y. Nakamura, C.J.P.M. Harmans, and H.J. Mooij, Science **299**, 1869 (2003).
 - [4] D. Vion, A. Aassime, A. Cottet, P. Joyez, H. Pothier, C. Urbina, D. Esteve, and M.H. Devoret, Science **296**, 886 (2002).
 - [5] J. Tobiska and Yu. V. Nazarov, Phys. Rev. Lett. **93**, 106801 (2004); E.B. Sonin, Phys. Rev. B **70**, 140506(R) (2004).
 - [6] U. Weiss, *Quantum Dissipative Systems*, (World Scientific, Singapore, 1999).
 - [7] J.S. Langer, Ann. Phys. (NY) **41**, 108 (1967).
 - [8] D. Waxman, A.J. Leggett, Phys. Rev. B **32**, 4450 (1985).
 - [9] H. Grabert, P. Olschowski, U. Weiss, Phys. Rev. B **36**, 1931 (1987).
 - [10] H. Grabert, U. Weiss, Z.Phys. B Condensed Matter **56**, 171 (1984).
 - [11] J.M. Martinis and H. Grabert, Phys. Rev. B **38**, 2371 (1988).
 - [12] E. Paladino, L. Faoro, G. Falci, and R. Fazio, Phys. Rev. Lett. **88**, 228304 (2002).
 - [13] Yu. Makhlin and A. Shnirman, Phys. Rev. Lett. **92**, 178301 (2004).
 - [14] D.J. Van Harlingen, T.L. Robertson, B.L.T. Plourde, P.A. Reichardt, T.A. Crane, and J. Clarke, Phys. Rev. B **70**, 064517 (2004).
 - [15] K. Rabenstein, V.A. Sverdlov, and D.V. Averin, cond-mat/0401519.
 - [16] E. Paladino, A. Mastellone, A.D'Arrigo, and G. Falci, cond-mat/0407484.
 - [17] P. Dutta and P.M. Horn, Rev. Mod. Phys. **53**, 497 (1981).
 - [18] A.B.Zorin, F.-J. Ahlers, J.Niemeyer, T.Weimann, H.Wolf, V.A.Krupenin and S.V.Lotkhov, Phys Rev. B **53**, 13682 (1996).
 - [19] J. Ankerhold and H. Grabert, Phys. Rev. Lett. **91**, 016803 (2003)
 - [20] G. Ithier, E. Collin, P. Joyez, D. Vion, D. Esteve, and J. Ankerhold and H. Grabert, submitted to Phys. Rev. Lett.
 - [21] P. Hänggi, P. Talkner, and M. Borkovec, Rev. Mod. Phys. **62**, 251 (1990).
 - [22] H. Grabert, P. Schramm und G.-L. Ingold, Phys. Rep. **168**, 115 (1988).
 - [23] J. Ankerhold and H. Grabert, Phys. Rev. E **61**, 3450 (2000) and references therein.
 - [24] J. Ankerhold and P. Pechukas, Europhys. Lett. **52**, 264 (2000).